Developmental Cell
Article

Tensin-4-Dependent MET Stabilization Is Essential for Survival and Proliferation in Carcinoma Cells

Ghaffar Muharram,[1,2,8] Pranshu Sahgal,[1,2] Taina Korpela,[3,4] Nicola De Franceschi,[1,2] Riina Kaukonen,[1,2] Katherine Clark,[5] David Tulasne,[6] Olli Carpén,[3,4] and Johanna Ivaska[1,2,7,*]
[1]Turku Centre for Biotechnology, University of Turku, Turku, 20520, Finland
[2]VTT Technical Research Centre of Finland, Turku, 20521, Finland
[3]Department of Pathology, University of Turku, Turku, 20520, Finland
[4]Department of Pathology, Turku University Hospital, Turku, 20520, Finland
[5]Department of Biochemistry, University of Leicester, Leicester LE1 9HN, UK
[6]Institut de Biologie de Lille-UMR8161, CNRS, 59021 Lille, France
[7]Department of Biochemistry and Food Chemistry, University of Turku, 20520, Finland
[8]Present address: Institut Curie-UMR144, Paris, France
*Correspondence: johanna.ivaska@utu.fi
http://dx.doi.org/10.1016/j.devcel.2014.03.024

SUMMARY

Inappropriate MET tyrosine kinase receptor signaling is detected in almost all types of human cancer and contributes to malignant growth and MET dependency via proliferative and antiapoptotic activities. Independently, Tensin-4 (TNS4) is emerging as a putative oncogene in many cancer types, but the mechanisms of TNS4 oncogenic activity are not well established. Here, we demonstrate that TNS4 directly interacts with phosphorylated MET via the TNS4 SH2-domain to positively regulate cell survival, proliferation, and migration, through increased MET protein stability. In addition, TNS4 interaction with β1-integrin cytoplasmic tail positively regulates β1-integrin stability. Loss of TNS4 or disruption of MET-TNS4 interaction triggers MET trafficking toward the lysosomal compartment that is associated with excessive degradation of MET and triggers MET-addicted carcinoma cell death in vitro and in vivo. Significant correlation between MET and TNS4 expression in human colon carcinoma and ovarian carcinoma suggests TNS4 plays a critical role in MET stability in cancer.

INTRODUCTION

The receptor tyrosine kinase (RTK) MET is activated by its ligand the hepatocyte growth factor (HGF) and is a potent regulator of morphogenesis and migration, during development and in response to tissue injury in the adult (Trusolino et al., 2010). MET activation induced by receptor overexpression, genetic amplification (Houldsworth et al., 1990), mutation (Peschard et al., 2001), or increased HGF secretion (Rong et al., 1994; Straussman et al., 2012) is frequently observed in cancer cells. HGF stimulation results in MET activation and subsequent phosphorylation of key tyrosine residues that regulate the recruitment of adaptor proteins (Trusolino et al., 2010), MET internalization (Peschard et al., 2001), transient endosomal signaling (Kermorgant et al., 2004), and MET receptor trafficking toward either degradation (Hammond et al., 2001) or recycling back to the membrane (Hammond et al., 2003; Parachoniak et al., 2011). In cancer, activating mutations in MET (Joffre et al., 2011) or gain-of-function mutants of p53 (Muller et al., 2013) induce sustained MET recycling, promoting tumorigenesis and invasion. Therefore, a better understanding of the mechanisms regulating MET turnover is critical.

RTK signaling is adhesion dependent under normal conditions, and crosstalk between integrin cell-adhesion receptors and RTKs, including MET, is well established (Ivaska and Heino, 2011; Lai et al., 2009). Tensins, a family of four scaffolding proteins (TNS1, TNS2, TNS3, and TNS4), are emerging as important regulators of cell motility and growth (Qian et al., 2009). Tensins 1–3 link integrins to actin via their PTB domains (Calderwood et al., 2003) and are important components of fibrillar adhesions (Clark et al., 2010; McCleverty et al., 2007). Interestingly, unlike other tensins, TNS4 expression is restricted within normal tissue (Chen et al., 2013; Lo and Lo, 2002). TNS4 promotes cell migration by triggering the uncoupling of integrins from the actin cytoskeleton (Katz et al., 2007) and is emerging as a putative oncogene in many cancer types (Albasri et al., 2009; Katz et al., 2007; Liao et al., 2009; Sakashita et al., 2008; Sasaki et al., 2003a, 2003b). However, the mechanisms underlying the oncogenicity of TNS4 are poorly described. All tensins are known to interact via their SH2 domains with tyrosine-phosphorylated cytoplasmic signaling molecules (Lo, 2007), such as FAK, PI3K, and p130Cas, but the functional relevance of these interactions is not fully elucidated (Cui et al., 2004; Defilippi et al., 2006; Mitra and Schlaepfer, 2006).

Here, we show a direct, tyrosine phosphorylation-dependent interaction between MET and TNS4 that occurs through the TNS4 SH2 domain and inhibits MET endocytosis and subsequent lysosomal degradation. TNS4 also regulates β1-integrin stability, MET-dependent cell migration, proliferation, and survival in vitro and functions as a critical determinant of "MET-addicted tumor" viability in vivo.

A

Gene Name	# of clones	SID	/functional domains
GAB1	20	AA 460-516	/MBD (Met binding domain)
GRB2	14	AA 57-216	/SH2 and C-terminal SH3
PLCG1	19	AA 616-662	/SH2
PIK3R1 variant 1	21	AA 411-498	/SH2
TNS3	5	AA 1135-1356	/SH2
TNS4	4	AA 416-624	/SH2

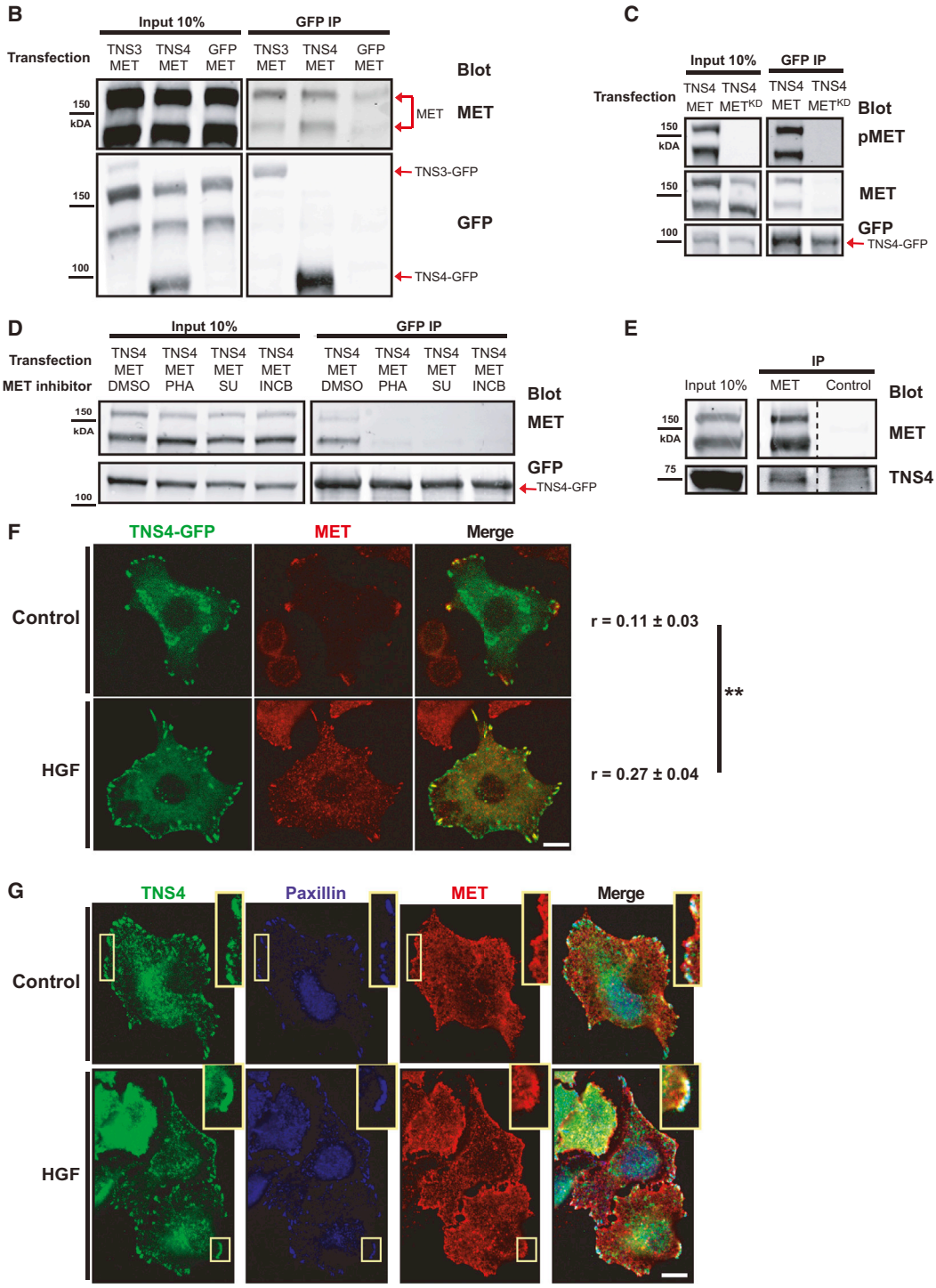

(legend on next page)

RESULTS

Tensin Isoforms 3 and 4 Associate with Active MET

Yeast two-hybrid screens using a truncated intracellular version of MET (containing its kinase domain) as bait revealed an interaction between tensin isoforms 3 and 4 and MET (Figure 1A). Several of the well-defined MET-interacting proteins (PI3K, GAB1, and GRB2 protein isoforms) were also identified, thus validating the approach. TNS3-GFP and TNS4-GFP, but not GFP alone, coimmunoprecipitated with overexpressed MET in HEK293 cells (Figure 1B). This interaction did not require HGF stimulation as the transiently overexpressed MET is constitutively phosphorylated in HEK293 cells, due to high expression levels (Figure S1A available online; note that both bands detected in the overexpressing cells represent phosphorylated MET bands). TNS4, unlike TNS3, lacks an actin-binding domain (Figure S1B) and has been suggested to possess oncogenic functions in many cancer types. This notion was further validated by our analysis of publicly accessible microarray data for changes in *TNS3* and *TNS4* gene expression. In colorectal, lung, ovarian, and gastric cancers, TNS4 was significantly upregulated with concomitant downregulation of TNS3 levels (Figure S1C) compared to normal tissue. Focusing on TNS4, we further confirmed that the association with MET was dependent on MET kinase activity (Figures 1C and 1D). TNS4-GFP coimmunoprecipitated phosphorylated MET, whereas expression of a kinase-dead mutant of MET (MET ^{KD}) or wild-type (WT) MET (MET ^{WT}) in combination with three different specific MET kinase inhibitors abolished TNS4-MET association. Consistent with the recruitment of TNS4 to MET in a phosphorylation-dependent manner, coimmunoprecipitation of endogenous MET and TNS4 (Figure 1E) was observed in GTL-16 gastric carcinoma cells harboring *MET* amplification and high levels of constitutively active MET. In A549 lung carcinoma cells, endogenous MET overlapped with TNS3-GFP, confirming their ability to associate as shown above (Figure S1D). Endogenous MET and TNS4-GFP (Figure 1F) localized to the same membrane structures and exhibited a significant increase in colocalization following HGF stimulation (Figure 1F and GFP-transfected control cells Figure S1E). Furthermore, endogenous TNS4 and MET overlapped in paxillin-positive adhesion sites (Figure 1G).

Active MET Binding to TNS4 SH2 Domain Requires the R474 Residue

To better define the TNS4-MET association, we generated a TNS4 C-terminal construct containing only the TNS4 SH2 and PTB domains (Figure 2A) and expressed this as a recombinant glutathione S-transferase (GST) fusion protein (Figure S2A). In pull-downs, a GST-TNS4-SH2-PTB fragment (but not GST alone; Figure S2B) was sufficient to pull down MET from HGF-responsive A549 cells (Figures 2B and 2C) with low basal HGF secretion (Figure S2C) and MET activity and from GTL-16 cells with *MET* amplification and high levels of the constitutively phosphorylated MET receptor (Figures 2B and 2C). TNS4-MET binding was dependent on MET activity; binding was induced by HGF stimulation in A549 cells and reduced in GTL-16 cells upon MET kinase inhibition (Figure 2C).

Next, we sought to identify the TNS4 MET binding site, which according to our yeast two-hybrid screen resides in the SH2 domain (Figure 1A). SH2 domains that bind phosphotyrosine (pY) motifs include a conserved arginine residue corresponding to arginine-175 in v-Src (Huang et al., 2008). Homology modeling of TNS4 SH2 domain superimposed on the v-Src SH2 domain, identified arginine-474 as a potential putative MET pY binding site (Figure 2D). Consistent with this prediction, substitution of arginine-474 with alanine (R474A), in the context of full-length TNS4-GFP, significantly decreased the MET-TNS4 association in cells coexpressing MET (Figure 2E). Thus, the association between phosphorylated MET and TNS4 depends on R474 in the SH2 domain of TNS4.

The TNS4 SH2 Domain Is Required for Binding MET on Y1313 and the Docking Site

MET recruits binding partners via key pY residues within its cytoplasmic domain (Figure 2F). To test whether the TNS4 SH2 domain directly interacts with MET, and to map the MET pY residue(s) required for TNS4 association (Figure S2D), we employed an in vitro ELISA binding assay (Garcia-Echeverria et al., 1997). Biotinylated MET phosphopeptides encompassing the juxtamembrane Y1003, the kinase domain Y1234-Y1235 (in combination), Y1313, the docking-site Y1349 and Y1356 (separately or in combination in one peptide), and Y1365 were tested for their ability to interact with recombinant GST-TNS4-SH2-PTB. MET peptides containing Y1003 and Y1365 demonstrated only residual binding to GST-TNS4-SH2-PTB. MET peptides encompassing Y1234-Y1235 and Y1349 exhibited intermediate binding, whereas peptides containing Y1313, Y1356, and the combination of Y1349 and Y1356 presented the strongest interaction with GST-TNS4-SH2-PTB (Figures 2F and 2G). We next compared a consensus pY recognition sequence reported for TNS4 SH2 domain binding (Huang et al., 2008) with the MET phosphopeptide sequences and with a previously reported

Figure 1. MET Associates with TNS3 and TNS4

(A) TNS3 and TNS4 were identified as putative MET interactors in a yeast two-hybrid screen using an intracellular kinase domain-containing fragment of MET. SID (selected interaction domain) indicates the common amino acid sequence that binds with the respective protein of interest. Functional domains in the SIDs are shown.

(B) GFP-TRAP pull-down in HEK293 cells cotransfected with MET and GFP or TNS3-GFP or TNS4-GFP.

(C) GFP-TRAP pull-down in HEK293 cells cotransfected with TNS4-GFP and MET or a kinase-dead mutant of MET (KD).

(D) GFP-TRAP pull-down in HEK293 cells cotransfected with TNS4-GFP and MET and treated with MET kinase inhibitors PHA (PHA665752, 300 nM), SU (SU1174, 5 μM), or INCB (INCB28060, 2 μM) for 16 hr.

(E) Endogenous MET immunoprecipitation from GTL-16 cell extracts compared to nonbinding immunoglobulin G (IgG) control immunoprecipitation.

(F) Representative single channel and merged images of TNS4-GFP and MET staining (antibody directed against intracellular domain) in control and HGF-treated (30 ng/ml, for 30 min) A549 cells expressing TNS4-GFP. r = Pearson's correlation coefficient between TNS4-GFP and MET staining in cells (mean ± SEM; n = 25 cells from three independent experiments; statistical significance was analyzed with Student's t test). Scale bar, 10 μm.

(G) Representative single channel and merged images of control and HGF-treated (30 ng/ml, for 30 min) A549 cells stained for endogenous TNS4, paxillin, and MET (antibody directed against extracellular domain). Insets highlight regions of colocalization. n = 3 independent experiments. Scale bar, 10 μm.

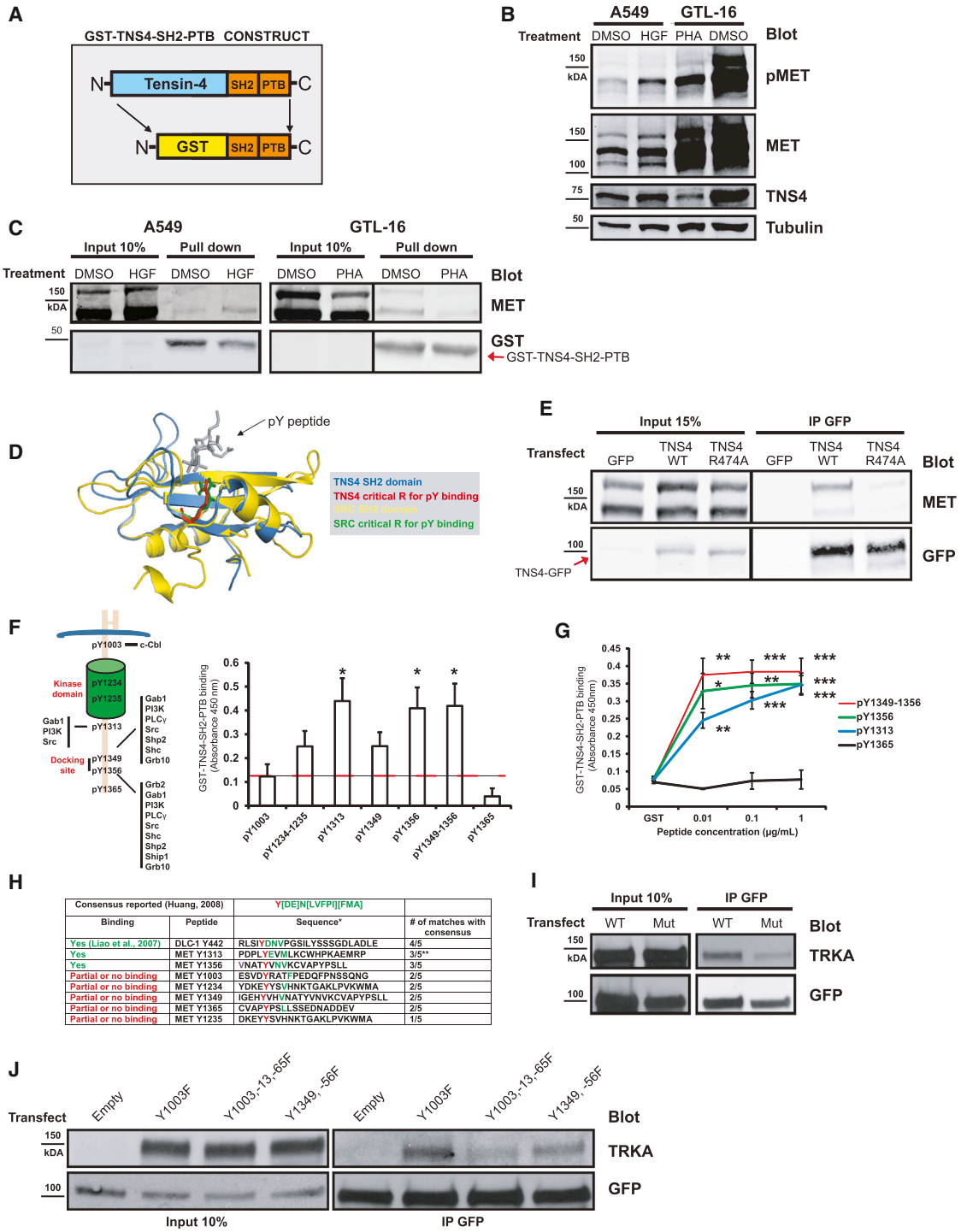

Consensus reported (Huang, 2008)		Y[DE]N[LVFPI][FMA]	
Binding	Peptide	Sequence*	# of matches with consensus
Yes (Liao et al., 2007)	DLC-1 Y442	RLSIYDNVPGSILYSSSGDLADLE	4/5
Yes	MET Y1313	PDPLYEVMLKCWHPKAEMRP	3/5**
Yes	MET Y1356	VNATYVNVKCVAPYPSLL	3/5
Partial or no binding	MET Y1003	ESVDYRATFPEDQFPNSSQNG	2/5
Partial or no binding	MET Y1234	YDKEYYSVHNKTGAKLPVKWMA	2/5
Partial or no binding	MET Y1349	IGEHYVHVNATYVNVKCVAPYPSLL	2/5
Partial or no binding	MET Y1365	CVAPYPSLLSSEDNADDEV	2/5
Partial or no binding	MET Y1235	DKEYYSVHNKTGAKLPVKWMA	1/5

Figure 2. TNS4 SH2 Domain Interacts with Several Phosphorylated Tyrosines in MET

(A) Schematic representation of recombinant GST fusion constructs containing TNS4 C terminus SH2 and PTB domains.

(B) A549 and GTL-16 cells treated as indicated with HGF (100 ng/ml, 15 min) or PHA (300 nM, 16 hr) and analyzed by western blot.

(C) Pull-down of MET with recombinant GST-TNS4-SH2-PTB from A549 or GTL-16 cell lysates treated as in (B).

(D) Model of TNS4-SH2 domain (blue) superimposed on the published Src SH2 domain crystal structure (yellow) in complex with a phosphotyrosine (pY) peptide (gray). The critical arginine in the Src SH2 domain required for pY-binding is indicated in green, and the predicted corresponding arginine residue in TNS4 (R474) is indicated in red.

(E) GFP-TRAP pull-down in HEK293 cells cotransfected with MET and TNS4-GFP or TNS4-GFP_R474A.

(legend continued on next page)

sequence of DLC-1 that also binds TNS4 SH2 domain (Liao et al., 2007). The results of our binding assays, i.e., the interaction affinity between MET and TNS4, correlated with the degree of sequence homology between the MET phosphopeptides and the consensus pY recognition motif reported for TNS4 SH2 domain (Figure 2H).

The TNS4-MET interaction was further validated in the cellular context. Transiently transfected TNS4-GFP associated with TRK-MET-WT (chimeric neurotrophin and MET receptor fusion) but failed to coimmunoprecipitate the TRK-MET mutant (Mut; bearing Y1313F, Y1349F, Y1356F, and Y1365F substitutions) (Figure 2I). The observed residual binding of TNS4 to the mutant receptor may be due to the intact MET kinase domain that is still present within the mutant construct that exhibited intermediate binding to TNS4 in our ELISA assays (Figures 2F and 2G). In correlation with the in vitro binding, phenylalanine substitution of Y1003 (TRK-MET-Y1003F) did not abolish the ability of TNS4-GFP to associate with the MET receptor, whereas mutation of Y1313 (TRK-MET-Y1003F,-Y1313F,-Y1365F) markedly reduced TNS4 binding to MET. Mutagenesis of the docking-site residues (TRK-MET-Y1349F,-Y1356F) also reduced TNS4 interaction (Figure 2J). Taken together, these data suggest that TNS4 binds preferentially to MET via the docking site and the less well-characterized Y1313 residue within MET.

TNS4, MET, and β1-Integrin Form Complexes

As TNS4-MET association requires the TNS4 SH2 domain (Figure 2), and as TNS4-β1-integrin interaction is known to occur through TNS4 PTB domain (adjacent to TNS4 SH2) (Calderwood et al., 2003; Katz et al., 2007), we hypothesized that these three proteins may form a complex to regulate cellular functions, such as cell migration. In A549 cells expressing TNS4-GFP, we observed overlap between TNS4-GFP, MET, and β1-integrin staining, particularly in adhesion sites (Figure 3A). In addition, endogenous MET, TNS4, and β1-integrin coimmunoprecipitated in HGF-stimulated A549 cells (Figure 3B) and recombinant GST-TNS4-SH2-PTB associated with both MET and β1-integrin (Figure 3C). The TNS4-β1-integrin complex was not dependent on growth factor stimulation, consistent with the ability of tensins to interact with both phosphorylated and nonphosphorylated β-integrin tails (Legate and Fässler, 2009). However, as expected HGF stimulation increased the recruitment of MET to TNS4 (Figure 3C).

As both β1-integrin and MET are strongly implicated in cell motility, we tested if TNS4 is involved in cell migration. Analysis of A549 cell migration on cell-derived matrices revealed a modest effect of TNS4 silencing on the basal migration of nonstimulated cells. However, loss of TNS4 fully abolished the HGF-induced cell motility as compared to control HGF-treated cells (Figure 3D; control small interfering RNA [siRNA] cells in Movie S1 and TNS4 siRNA cells in Movie S2). Importantly, reintroduction of an siRNA-resistant TNS4-GFP, and not GFP alone (see Figure 4B for siRNA D efficiency), restored cell migration comparable to levels seen in control cells. Moreover, expression of TNS4-GFP alone was sufficient to increase cell migration in control siRNA-transfected cells (Figure 3E). Importantly, the ability of TNS4 to interact with MET was critical for cell migration as expression of the TNS4 MET-binding mutant (TNS4_R474A-GFP) significantly inhibited basal and more notably HGF-stimulated A549 cell migration (Figure 3F).

TNS4 Positively Regulates MET Levels and Downstream Signaling

Unexpectedly, we observed that MET and β1-integrin total protein levels were reduced upon TNS4 silencing (Figure 4A; TNS4 smartpool siRNA [four oligos] and a single independent 3′ UTR RNAi oligo), without significant reduction in the corresponding transcription levels (quantitative real-time PCR measurements; mean Rq values ± SD fold changes: 1.04 ± SD 0.33 and 1.03 ± 0.45, respectively, for β1 and MET in TNS4- versus control-silenced cells, n = 2), indicative of protein level regulation. TNS4 silencing reduced total β1-integrin levels by 26%–55% (Figure 4A) and cell-surface β1-integrin expression (Figure S3A). In contrast, β1-integrin silencing did not influence TNS4 expression (Figure S3B). Furthermore, this effect was specific to TNS4 as TNS3 downregulation did not markedly affect MET or β1-integrin levels (Figure S3B). The effect of TNS4 silencing on MET expression was even more pronounced. TNS4 smartpool siRNA (four oligos) or a single RNAi oligo (siD) (resulting in a 40%–52% and 41% reduction in TNS4 expression, respectively) led to a significant downregulation of MET protein expression (28% and 59%, respectively as compared to control cells) (Figure 4B). As expected, TNS4 silencing significantly reduced MET cell-surface expression (Figure 4C) and influenced MET downstream signaling. In correlation with decreased MET levels, ligand-induced MET activation (pMET levels, 30 min HGF) was impaired together with a 54% reduction in Akt activation compared to HGF-stimulated control cells (Figure 4D). TNS4-silencing reduced Akt activation also after 1 or 2 hr HGF stimulation (Figure S3C). Interestingly, HGF induced a modest activation of ERK with no significant difference in ERK activity between control and TNS4 siRNA cells (Figure S3C). Hence, these data demonstrate a requirement for TNS4 in the maintenance of β1-integrin and MET protein levels and HGF-induced signaling. However, the ability of TNS4 to support expression of both receptors is unlikely to be related to the formation of

(F) Schematic representation of key MET tyrosines and respective known interactors. Right panel depicts in vitro ELISA binding assay of GST-TNS4-SH2-PTB with biotinylated MET phosphopeptides (mean absorbance ± SEM; n = 4; statistical significance in comparison with nonbinding pY1365 peptide was analyzed with Student's t test).

(G) Dose-dependent binding of phosphopeptides to GST-TNS4-SH2-PTB (mean absorbance ± SEM; n = 3; statistical significance in comparison with nonbinding pY1365 peptide).

(H) pY sequence alignment highlighting consensus binding site with TNS4 SH2 domain (Huang et al., 2008). (*For the full peptide sequence, see Table S1. **Because methionine is commonly considered a bulky hydrophobic residue, we regarded it as matching with the consensus.)

(I) TNS4-GFP (transiently transfected) coimmunoprecipitation from MDCK cells stably overexpressing TRK-MET-WT or mutated construct TRK-MET-Y1313F, Y1349F, Y1356F, Y1365F (Mut).

(J) TNS4-GFP coimmunoprecipitation from HeLa cells transiently overexpressing TNS4-GFP and TRK-MET constructs mutated on Y1003 (Y1003F) or Y1003, Y1313 and Y1365 (Y1003,-13,-65F) or Y1349 and Y1356 (Y1349, −56F) or empty control construct. *$p < 0.05$, **$p < 0.005$, ***$p < 0.001$.

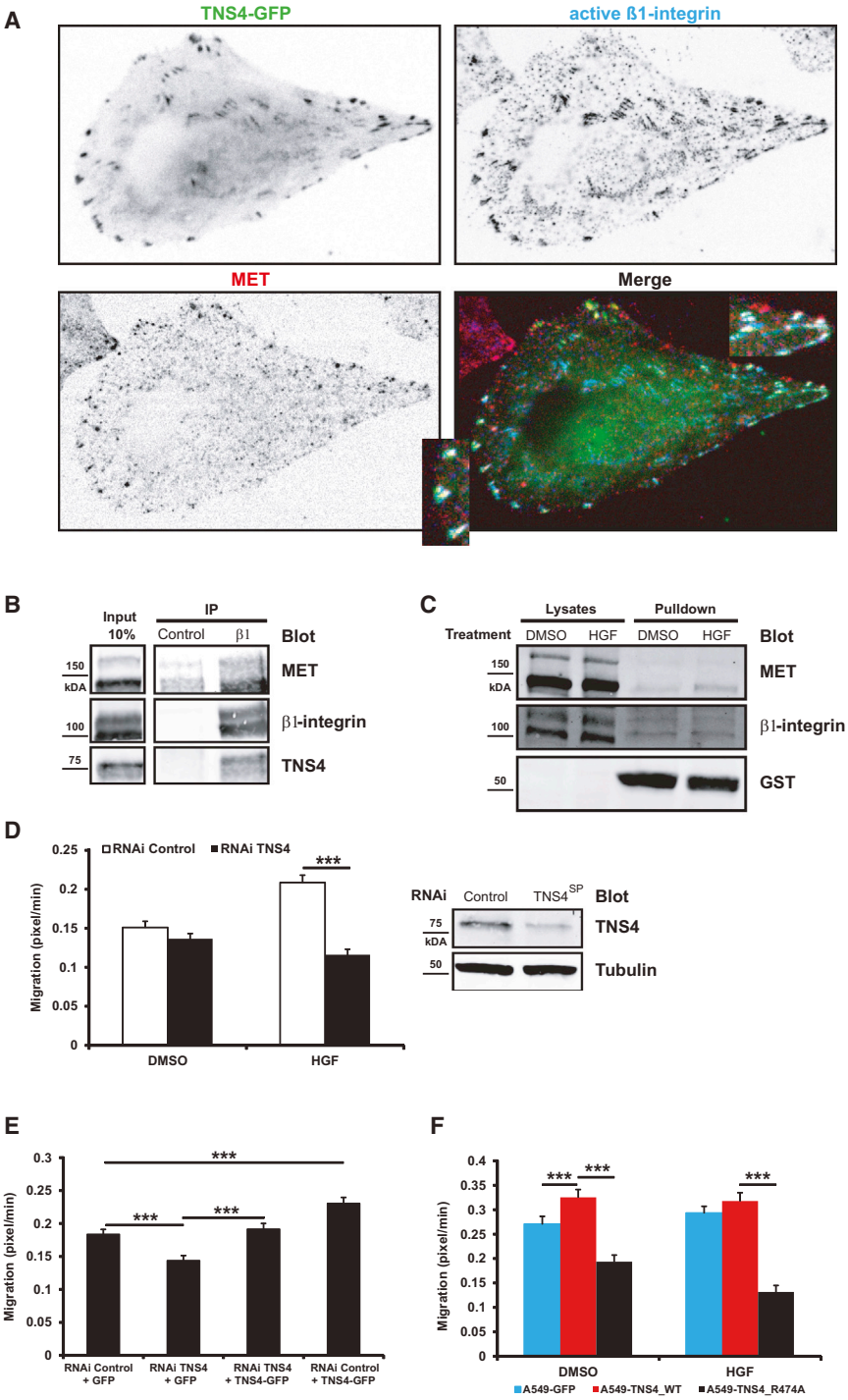

Figure 3. TNS4, MET, and β1-Integrin Form Complexes Influencing A549 Cell Migration

(A) Active β1-integrin (9EG7) and MET (antibody directed against intracellular domain) staining of A549 cells overexpressing TNS4-GFP, plated on fibronectin, and treated with HGF (30 ng/ml, 30 min). Insets highlight areas of overlap between the three channels. Shown are inverted single channel images and a merged representative of three independent experiments. Scale bar, 10 μm.

(B) Coimmunoprecipitation of MET, TNS4, and β1-integrin from cells treated with HGF (10 ng/ml, 16 hr).

(C) Pull-down of MET and β1-integrin with GST-TNS4-SH2-PTB from whole-cell lysates ± HGF (100 ng/ml, 15 min).

(D) Migration of control- or TNS4-silenced (100 nM, smart pool [SP] of four oligos) A549 cells ± HGF (10 ng/ml), on cell-derived matrices (mean speed ± SEM of 190 cells tracked for 12 hr; n = 3). Cell lysates were analyzed for TNS4 silencing efficiency, and tubulin was used as loading control.

(E) Migration of control- or TNS4-silenced (100 nM, single RNAi oligo D; described in Figure 4B) A549 cells expressing GFP or TNS4-GFP resistant to RNAi oligo D on cell-derived matrices (mean speed ± SEM of 150 cells tracked for 12 hr; n = 3).

(F) Migration of A549 cells overexpressing GFP, TNS4-GFP_WT, or TNS4-GFP_R474A constructs, ± HGF (10 ng/ml), on cell-derived matrices (mean speed ± SEM of at least 70 cells tracked for 12 hr; n = 3).

Statistical significance was analyzed by Student's t test. ***$p < 0.0001$ (D–F).

the MET-β1-integrin-TNS4 complex as β1-integrin silencing had no effect on MET levels (Figure S3B). Careful observation of the data also revealed a possible feedback loop between MET and TNS4 expression. HGF stimulation significantly increased TNS4 levels (approximately 40%) (Figure S3C), with a modest increase already detectable after 30 min (Figure 4D and S3D). Correspondingly, in MET overexpressing GTL-16 cells pharmacological inhibition of MET activity reduced endogenous TNS4 levels by 64% (Figure S3D), suggesting a reciprocal positive regulatory loop between MET and TNS4.

TNS4 Regulates MET Stability

Ligand-induced activation of MET and subsequent MET receptor internalization, degradation, and/or recycling is well established (Parachoniak et al., 2011). Recent studies have demonstrated that under basal, non-HGF-induced conditions, several mechanisms may regulate the half-life of the MET receptor independently of ligand binding (Lefebvre et al., 2012). We investigated whether TNS4 could contribute to the steady-state turnover of MET in cells. MET levels remained nearly unaltered in TNS4_WT-GFP-expressing cells treated with cycloheximide but were clearly reduced in GFP cells (Figure 4E). A similar pattern was detected in total MET levels analyzed by western blot (Figure S4A). The ability of TNS4 to stabilize MET was dependent on the TNS4-MET interaction as expression of the MET-binding-defective mutant, TNS4_R474A-GFP, significantly increased MET turnover compared to TNS4_WT-GFP (Figure 4F). In addition, the C terminus of TNS4 was sufficient for MET stabilization as

reintroduction of TNS4-SH2-PTB lacking the RNAi B target sequence was able to rescue cell-surface MET levels in TNS4-silenced cells (Figure 4G).

The difference in protein stability suggested a possible role in receptor trafficking, as ligand-activated MET is predominantly degraded following internalization. Using the well-established cell-surface biotinylation-based endocytosis assay (Mai et al., 2011; Roberts et al., 2001), we observed that in A549 cells, MET was constantly endocytosed, even in the absence of HGF (Figure 4H), most likely due to the low-level basal phosphorylation of MET present in these cells (Figure 2B). Silencing of TNS4 clearly increased MET endocytosis but had no significant effect on basal recycling of endocytosed MET (Figures 4H, S4B, and S4C; note that twice as much input lysate was used for siTNS4 cells to achieve comparable levels of MET immunoprecipitation). This was validated further by the finding that in cells overexpressing TNS4, the basal and HGF-induced endocytosis of MET was slower compared to control GFP cells (Figure 5A). The role of TNS4 in regulating MET internalization was validated further with another endocytosis assay employing antibody labeling and fluorescence-activated cell sorting (FACS) analysis. The data show that TNS4_WT-GFP expression significantly reduced the loss of cell-surface MET compared to GFP cells. Conversely, expression of the MET-binding mutant, TNS4_R474A-GFP, functioned in a dominant-negative fashion (similar to TNS4 siRNA) to augment MET uptake from the cell membrane (Figure 5B). Thus, TNS4 binding to MET functions to reduce MET endocytosis and retain MET on the membrane, both under basal, low MET activity and HGF-stimulated conditions. Recently, GGA3 was shown to be critical for MET stability by regulating MET recycling to the plasma membrane upon HGF stimulation (Parachoniak et al., 2011). In line with these data, we find that GGA3 silencing has no effect on MET levels under basal conditions but significantly increases HGF-induced MET downregulation. In contrast, TNS4 silencing reduces MET levels, both in control and HGF-stimulated cells (Figures 5C and S4D), further confirming that TNS4 regulates MET traffic at the level of endocytosis and that receptor recycling is regulated by GGA3 as shown previously (Parachoniak et al., 2011).

We also observed a modest reduction in integrin endocytosis in TNS4_WT-GFP-expressing cells under basal conditions (Figure 5D). This could be linked to the obvious cotrafficking of cell-surface-derived active β1-integrin and MET that was observed upon HGF induction (Figure 5E).

TNS4 Inhibits MET Trafficking toward a Lysosomal Compartment

Next, we examined the localization of MET in the presence of TNS4_WT-GFP or the binding-incompetent TNS4_R474A-GFP mutant, both transiently expressed with lysosomal marker Lamp1-RFP (Figures 5F and S5A). We observed faster MET trafficking toward the lysosomal compartment in TNS4_R474A mutant-expressing cells compared to TNS4_WT cells, especially following 10 min of ligand stimulation. In line with this, after 30 min, very little MET remained detectable in the TNS4_R474A-expressing cells compared to the much higher MET signal residing in the Lamp-1 vesicles of TNS4_WT cells (Figure S5A). The loss in intracellular MET staining upon TNS4 silencing was rescued with bafilomycin, a lysosomal inhibitor (Figure S5B). Interestingly, in control-silenced cells, with lower basal MET endocytosis, bafilomycin clearly increased focal adhesion-type localization of MET at the plasma membrane. However, this phenomenon remains to be investigated in future studies. Taken together, the presence of functional TNS4 protects MET from degradation under basal conditions and affects MET lysosomal targeting upon HGF stimulation.

TNS4 and MET Expressions Correlate in Colorectal and Ovarian Tumors

Human colorectal and ovarian cancers exhibit typically high MET expression (Birchmeier et al., 2003; Zhou et al., 2008). In addition, TNS4 has been identified as an oncogene in colorectal cancer (Albasri et al., 2009; Liao et al., 2009). Our data indicate that TNS4 levels correlate with MET protein stability in cell lines. To investigate whether this is applicable in vivo, we stained for TNS4 and MET in human tumor specimens. From a large cohort (Ålgars et al., 2011) of metastatic or locally advanced colorectal cancers, ten were selected because of their strong MET immunoreactivity in invasive areas and heterogeneous overall staining in the tumor. Independent scoring of staining intensity, in 80 areas of serial histology sections, demonstrated a significant correlation between MET and TNS4 staining within the same regions of the tumor ($p < 0.0001$) (Figure 6A).

Next, an ovarian tumor tissue microarray containing 196 tumor cores was stained for MET and TNS4 (Figure 6B). Whereas all tumor cores were immunoreactive for TNS4, 17 cases showed no staining for MET. TNS4 showed weak expression in 32 cases, moderate expression in 99 cases, and intense expression in 65 cases. MET staining was weak in 54 cases, moderate in 61 cases, and intense in 64 cases. The level of TNS4 and MET immunoreactivity correlated significantly ($p < 0.0001$) when all tumor cores were studied from adjacent histology slices from the same samples (Figure 6B). After exclusion of benign and borderline tumors from the analysis, the correlation remained significant ($p < 0.0001$). However, differences between histological subtypes of carcinomas were observed. In high-grade serous carcinomas ($n = 49$; $p < 0.0001$) and in mucinous carcinoma ($n = 39$; $p = 0.012$), TNS4 and MET staining correlated significantly. In endometrioid cystadenocarcinoma ($n = 43$; $p = 0.13$) such a correlation was not seen, suggesting that in some tumor types the regulatory activity of TNS4 on MET expression may be overcome by alternative pathways. Taken together, these data implicate TNS4 as a potential regulator of MET levels in human cancer.

TNS4 Is Required for MET-Induced Survival In Vitro and In Vivo

Both HGF/MET signaling and integrin-mediated cell adhesion regulate cell proliferation. By using the IncuCyte-automated incubator-microscope system (Haapa-Paananen et al., 2012), we observed a clear reduction in cell proliferation following TNS4 silencing (Figures 7A and S6A), correlating with reduced MET and β1-integrin levels in TNS4-silenced cells. However, the antiproliferative effect of TNS4 silencing is most likely linked to MET downregulation. Indeed, MET silencing abolished cell proliferation, whereas silencing of β1-integrin had no significant effect (Figures S6A and S6B). The effect of TNS4 silencing on cell proliferation (Figure 7B) was rescued with the concomitant

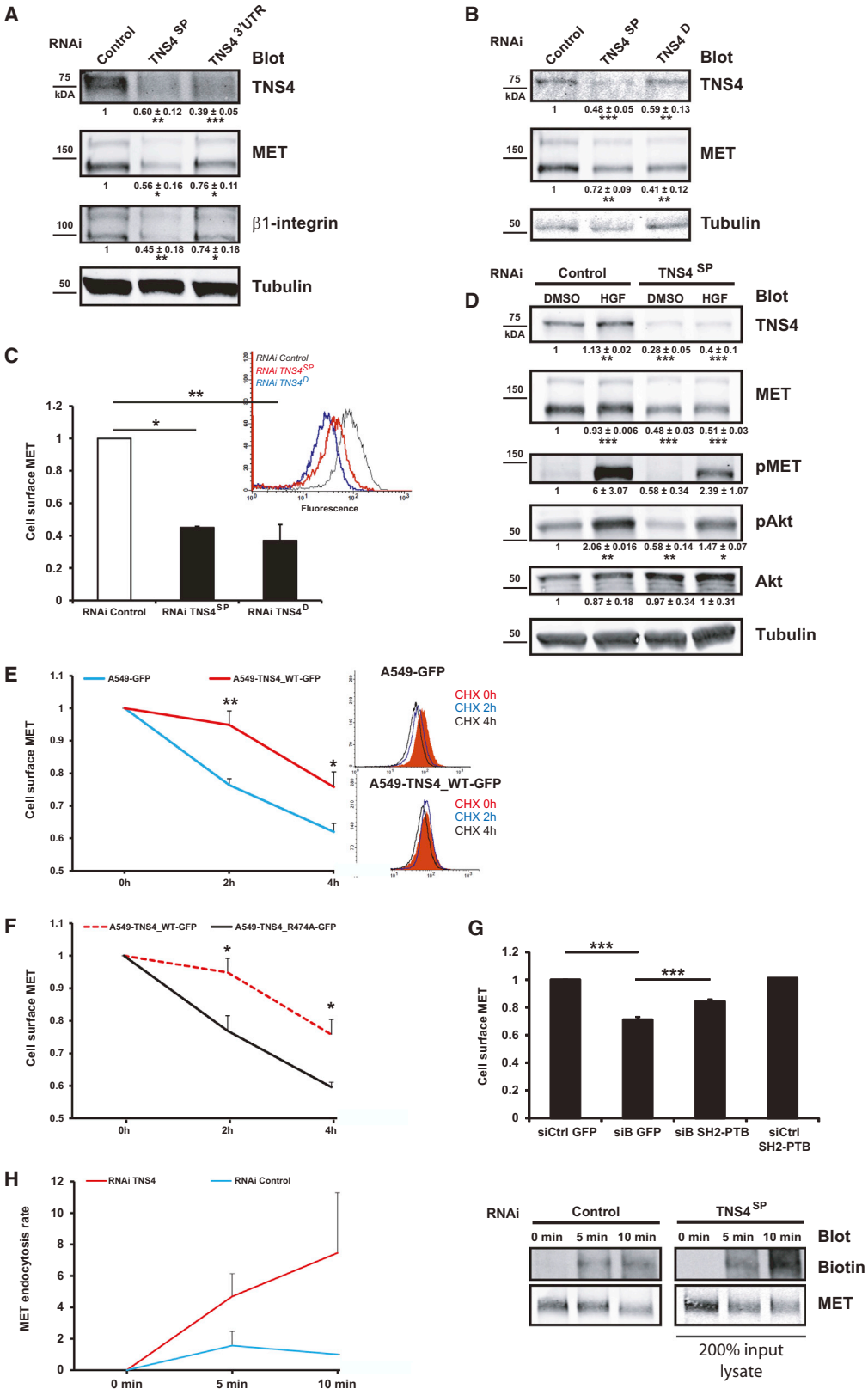

(legend on next page)

expression of a construct containing only TNS4 SH2-PTB and lacking the RNAi B target sequence, demonstrating the specificity of TNS4 silencing on cell proliferation.

In a subset of cancers, *MET* is amplified, resulting in increased proliferation and dependence of cells on MET signaling in the form of oncogene addiction (Lutterbach et al., 2007). We investigated the effect of TNS4 silencing in three carcinoma cell lines with *MET* amplification (resulting in constitutively active MET) and in another cell line with lower levels of MET (and no basal MET activity): MET-addicted EBC-1 lung carcinoma, MKN-45 and GTL-16 gastric carcinoma cells, and nonaddicted OVCAR3 ovarian carcinoma cell line (Figure S6C). All of these cell lines expressed TNS4 (Figures 7C, 7D, and S6D), and similar to A549 cells, TNS4-silencing resulted in MET downregulation and a significant reduction in proliferation in the active MET-expressing cells (Figures 7D and S6D). However, in OVCAR3 cells, TNS4 silencing significantly affected MET downregulation and cell proliferation only in the presence of constant HGF stimulation (Figure 7C). These data demonstrate a MET-activity dependence for TNS4 in regulating MET-induced cell growth in different cell lines representing several cancer types. In cell lines with *MET* amplification (Lutterbach et al., 2007), including GTL-16 (Smolen et al., 2006), MET downregulation halts proliferation, ultimately resulting in apoptosis. Accordingly, we detected increased apoptosis in GTL-16 and MKN-45 cells upon suppression of TNS4 expression (Figures 7E and S6E).

To experimentally validate these data in vivo, control- and TNS4-silenced GTL-16 cells were grafted subcutaneously into nude mice to generate tumors in vivo (Bertotti et al., 2010). Consistent with the observed MET dependence of GTL-16 cells in vitro, tumors derived from TNS4-silenced GTL-16 cells were predominantly necrotic with only marginal areas of viable cells. This was in stark contrast to the control RNAi GTL-16 tumors in which the majority of the cells were viable (Figure 7F). Residual Ki67 and excessive terminal deoxynucleotidyl transferase dUTP nick end labeling (TUNEL) staining in TNS4-silenced tumor sections confirmed reduced viability compared to the control-silenced tumors (Figure 7G). Immunohistochemistry staining further revealed that the remaining small areas of viable cells in the TNS4 RNAi-treated tumors were in fact positive for TNS4, MET, and pMET (Figure S6F), suggesting that these viable tumor areas may have arisen from the subpopulation of nontargeted cells that are always present in RNAi-silenced cell populations. These data demonstrate that TNS4 is necessary for MET-dependent cancer cell proliferation and survival in vitro and in vivo.

DISCUSSION

The MET interactome has been studied extensively in recent years and many proteins facilitating MET downstream signaling have been identified (Gherardi et al., 2012). In this study, we provide evidence for a previously unidentified direct interaction between MET and TNS4. We further dissect how TNS4 regulates the stability of MET at the protein level, thus promoting MET prosurvival activity both in vitro and in vivo (summarized in Figure 7H).

Although many of the details of HGF-induced MET trafficking are well known (Hammond et al., 2001; Peschard et al., 2001), the precise mechanisms regulating turnover of this receptor in human carcinomas remain unidentified. We find that MET protein stability is critically regulated by the ability of the receptor to couple to the intracellular scaffold protein TNS4, recently described as an oncogene in multiple cancer types. TNS4 expression inhibits MET endocytosis and correlates with increased MET levels and protein stability. Conversely, introduction of a defective MET-binding TNS4 mutant or TNS4 silencing increases MET endocytosis, lysosomal targeting, and degradation, thus significantly reducing MET levels. Consistent with these in vitro data, examination of human colonic and ovarian tumors, where MET overexpression has been correlated with poor outcome (reviewed in Blumenschein et al., 2012), revealed a high degree of conformity between MET and TNS4 immunoreactivity, suggesting coregulation of MET and TNS4 in vivo.

A previous study described a critical role for the intact TNS4 SH2 domain in the developmental process of HGF-induced tubulogenesis. However, the critical molecular interactions mediated by the TNS4 SH2 domain were not investigated in detail in that study (Kwon et al., 2011). Interestingly, we demonstrate that TNS4 interacts with several phosphorylated tyrosines on MET, namely, Y1349 and Y1356, which form the multifunctional docking site (Trusolino et al., 2010) and with the less well-characterized Y1313. As TNS4 plays a fundamental role in MET stabilization, the existence of multiple TNS4 binding sites is not surprising and would potentially allow TNS4 binding even if Y1313 or the docking site are monopolized by other MET-binding downstream effectors.

Figure 4. TNS4 Regulates MET Stability

(A) A549 cells transfected with control or TNS4 siRNAs (100 nM SP or a single RNAi oligo in 3′ UTR end) and analyzed by western blot (mean ± SEM band intensity normalized to tubulin and relative to control-silenced cells; n = 3 independent experiments).

(B) Representative western blot showing TNS4 and MET reduction (analyzed as in A) in A549 cells following TNS4 silencing with SP or RNAi oligo D.

(C) FACS analysis of MET cell surface levels in A549 cells treated with control or TNS4 SP RNAi or TNS4 RNAi D (mean fluorescence intensities ± SD, normalized to control-silenced cells; n = 3). Lower panel shows representative FACS histograms.

(D) Western blot analysis of MET, pMET, pAkt, and Akt levels in control- or TNS4-silenced (SP) A549 cells treated with DMSO (control) or HGF as indicated (50 ng/ml, 30 min) (mean ± SEM band intensity normalized to tubulin and relative to control-silenced DMSO-treated cells; n = 3).

(E) FACS analysis of MET cell-surface levels in A549-TNS4_WT-GFP and control A549-GFP cells treated with cycloheximide (10 μg/ml) for the indicated times. Shown are representative histograms and quantifications (mean values ± SEM normalized to 0 hr time points; n = 3).

(F) Cell-surface MET levels compared in A549-TNS4_R474A-GFP and A549-TNS4_WT-GFP cells as described in (E).

(G) FACS analysis of MET cell surface levels in control- or TNS4 (siB)-silenced A549 cells expressing GFP or GFP-TNS4-SH2-PTB fragment (resistant to siB). Cells were allowed to endocytose MET for 30 min (mean ± SEM fluorescence intensity; n = 3).

(H) Endocytosis rate of biotinylated cell-surface MET in control- and TNS4 (SP)-silenced A549 cells ± HGF (30 ng/ml). Representative blots are shown (mean ± SEM band intensity normalized to end point [10 min]), relative to control-silenced cells. Lysate input in TNS4 (SP) cells equivalent to 200% of control input (n = 3). Statistical significance was analyzed by Student's t test. *$p < 0.05$, **$p < 0.005$, ***$p < 0.0005$ (A–G).

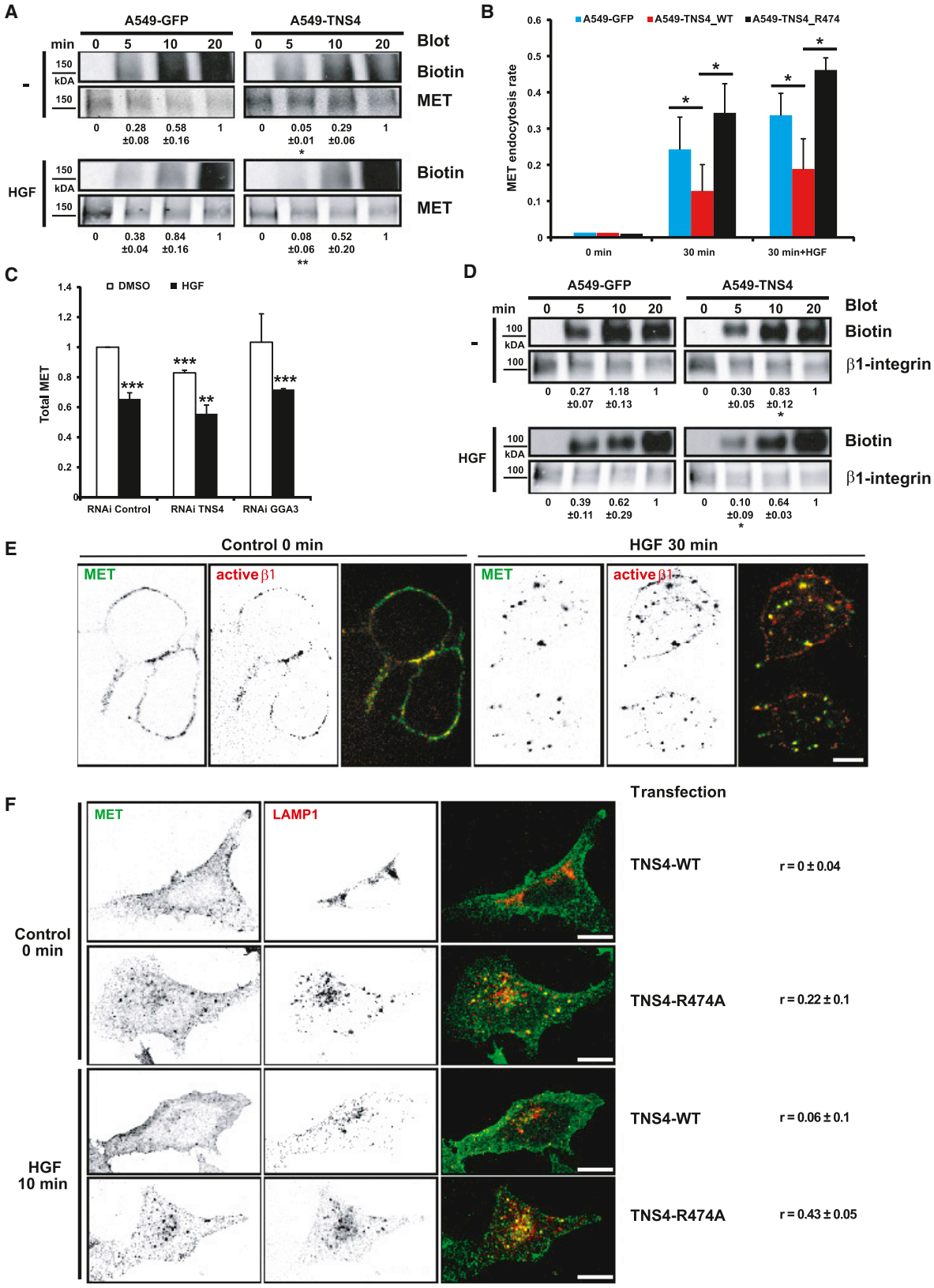

(legend on next page)

Our data demonstrate that in addition to increased MET gene expression, frequently detected in cancer (Zou et al., 2007), MET protein levels are controlled by TNS4. Hence, the ability of TNS4 to stabilize MET delineates an additional important level of MET regulation. Interestingly, we find a positive feedback loop between MET signaling and TNS4 through which HGF stimulation increases TNS4 levels and MET inhibition has the opposite effect. These data support the role of HGF in inducing TNS4 in MDCK cells (Kwon et al., 2011). We further observed that TNS4 levels are linked to increased β1-integrin stability and there are several cancer types, including breast cancer, in which elevated integrin expression is linked to poor prognosis (Goodman and Picard, 2012). The ability of TNS4 to regulate the endocytosis of and to stabilize MET and integrins is most likely one of the mechanisms whereby TNS4 mediates oncogenicity.

TNS4 was very recently implicated in stabilization of EGFR following EGF stimulation (Hong et al., 2013) and is transcriptionally regulated by EGFR signaling in mammary epithelial cells (Katz et al., 2007) and by BRAF in KRAS-mutated colorectal cancers (Al-Ghamdi et al., 2011). These data suggest that TNS4 could function not only as a regulator of several RTKs but also as an important node linking distinct oncogenic pathways in cancer cells. Here, we describe TNS4 as an important regulator of MET protein stability and MET-dependent cell survival. It is also possible that TNS4 couples EGFR or BRAF signaling to MET stability; however, this remains to be investigated.

In conclusion, our study demonstrates a direct interaction between MET and TNS4 that influences MET stability and regulates survival of MET-dependent carcinomas in vitro and in vivo. TNS4 supports prolonged MET plasma membrane localization, thus sustaining MET oncogenic signaling, and the significant coexpression of MET and TNS4 in ovarian and colon carcinomas suggests that this interaction is of putative clinical importance.

EXPERIMENTAL PROCEDURES

Cell Lines and DNA Constructs

For cell lines, culture conditions, and DNA constructs, see the Supplemental Experimental Procedures.

Antibodies and Reagents

Antibodies, RNAi oligomers, and phosphopeptides used are listed in the Supplemental Experimental Procedures. HGF, NGF, and cycloheximide were purchased from Sigma. PHA665752, SU1174, and bovine plasma fibronectin were purchased from Calbiochem, and INCB28060 was purchased from Selleckchem.

Yeast Two-Hybrid

The yeast two-hybrid screen was performed by Hybrigenics using human MET (amino acids 1003–1376) as bait on a human placenta cDNA library.

DNA and RNAi Transfections

DNA construct and siRNA transfections were carried out using Lipofectamine 2000 (Life Technologies) or HiPerFect (QIAGEN) according to the manufacturer's instructions.

Immunoprecipitation and Western Blotting

See Supplemental Experimental Procedures.

Phosphopeptide Binding Assay

The in vitro ELISA binding assay was adapted from Garcia-Echeverria et al. (1997). For further details and for modeling of TNS4 SH2 domain binding to phosphotyrosine peptide, see the Supplemental Experimental Procedures.

Microscopy and Image Analysis

See the Supplemental Experimental Procedures.

FACS Analysis

Cells were detached with HyQ Tase (HyClone) and fixed with PBS containing 2% PFA for 15 min at room temperature. Cell-surface MET was stained with MET-extracellular antibody (1/100 from R&D) for 1 hr at 4°C. After washing once with PBS, Alexa Fluor-conjugated secondary antibody was added and incubated for 1 hr at 4°C. Samples were analyzed with FACS array (Becton Dickinson). The mean fluorescent intensity was determined from 10,000 or 20,000 counted events. For the FACS-based endocytosis assay, adherent cells were labeled with nonstimulating extracellular domain-binding MET antibody (1:500, Ebioscience) on ice for 30 min. Unbound antibody was washed away, and the cells were chased in warm medium in the presence or absence of 30 ng/ml HGF. Cells were washed with cold PBS and carefully collected by scraping. Cells were fixed for 10 min at 4°C with 4% PFA, washed, and suspended in PBS followed by Alexa-647 conjugated secondary antibody staining and FACS analysis.

Biotin IP-Based Internalization and Recycling Assay

MET and β1-integrin endocytosis and MET recycling rates were measured using a cell-surface biotinylation-based assay as previously described (Arjonen et al., 2012). Briefly, cells were grown to 80% confluence, placed on ice, and washed once with cold PBS, and cell-surface proteins were labeled with 0.5 mg/ml of EZ-link cleavable sulfo-NHS-SS-biotin (#21331; Thermo Scientific) in Hanks' balanced salt solution (H9269; Sigma) for 30 min at 4°C. Unbound biotin was removed, and cells were washed with cold media and allowed to internalize receptors in prewarmed 10% serum-containing medium at 37°C for the indicated times. Cells were then quickly placed back on ice with the addition of cold media. The remaining biotin at the cell surface was removed with 60 mM MesNa (63705; sodium 2-mercaptoethanesulfonate: Fluka) in MesNa buffer (50 mM Tris-HCl [pH 8.6], 100 mM NaCl) for 30 min at 4°C, followed by quenching with 100 mM iodoacetamide (IAA, Sigma) for 15 min on ice. To detect the total surface biotinylation, one of the cell dishes was left on ice after biotin labeling and did not undergo internalization or

Figure 5. TNS4-MET Interaction Attenuates MET Internalization and Lysosomal Targeting

(A) Endocytosis rate of biotinylated cell-surface MET in A549-TNS4_WT-GFP and control A549-GFP cells ± HGF (30 ng/ml) (mean ± SEM band intensity normalized to end point [20 min]; n = 3). Statistical differences at each time point between GFP- and TNS4_WT-GFP-overexpressing cells were analyzed by Student's t test.

(B) FACS analysis of cell-surface MET endocytosis rate in A549-GFP, A549-TNS4_WT-GFP, or A549-TNS4_R474A-GFP cells ± HGF (30 ng/ml, 30 min) (mean ± SEM fluorescence intensity; n = 3).

(C) Total MET levels in control-, TNS4-, and GGA3-silenced A549 cells treated with DMSO or HGF (30 ng/ml, 1 hr) (mean ± SEM band intensity normalized to control-silenced cells; n = 3). Statistical significance was analyzed between control-silenced cells and the other conditions.

(D) Endocytosis rate of biotinylated cell-surface β1-integrin was measured as described in (A).

(E) MET and active β1-integrin coendocytosis upon HGF induction (30 ng/ml) in A549 cells labeled with cell-surface-bound MET (antibody directed against extracellular domain) and β1-integrin (12G10) antibodies. Scale bar, 10 μm.

(F) A549 cells cotransfected with TNS4 _WT-GFP or TNS4_R474A-GFP mutant and Lamp1-RFP were stained for MET (antibody directed against extracellular domain) after HGF (30 ng/ml) induction. r: Pearson's correlation coefficient between Lamp1-RFP and MET staining in cells (mean ± SEM; n = 7 cells per condition). Scale bar, 10 μm. *$p < 0.05$, **$p < 0.005$, ***$p < 0.0005$.

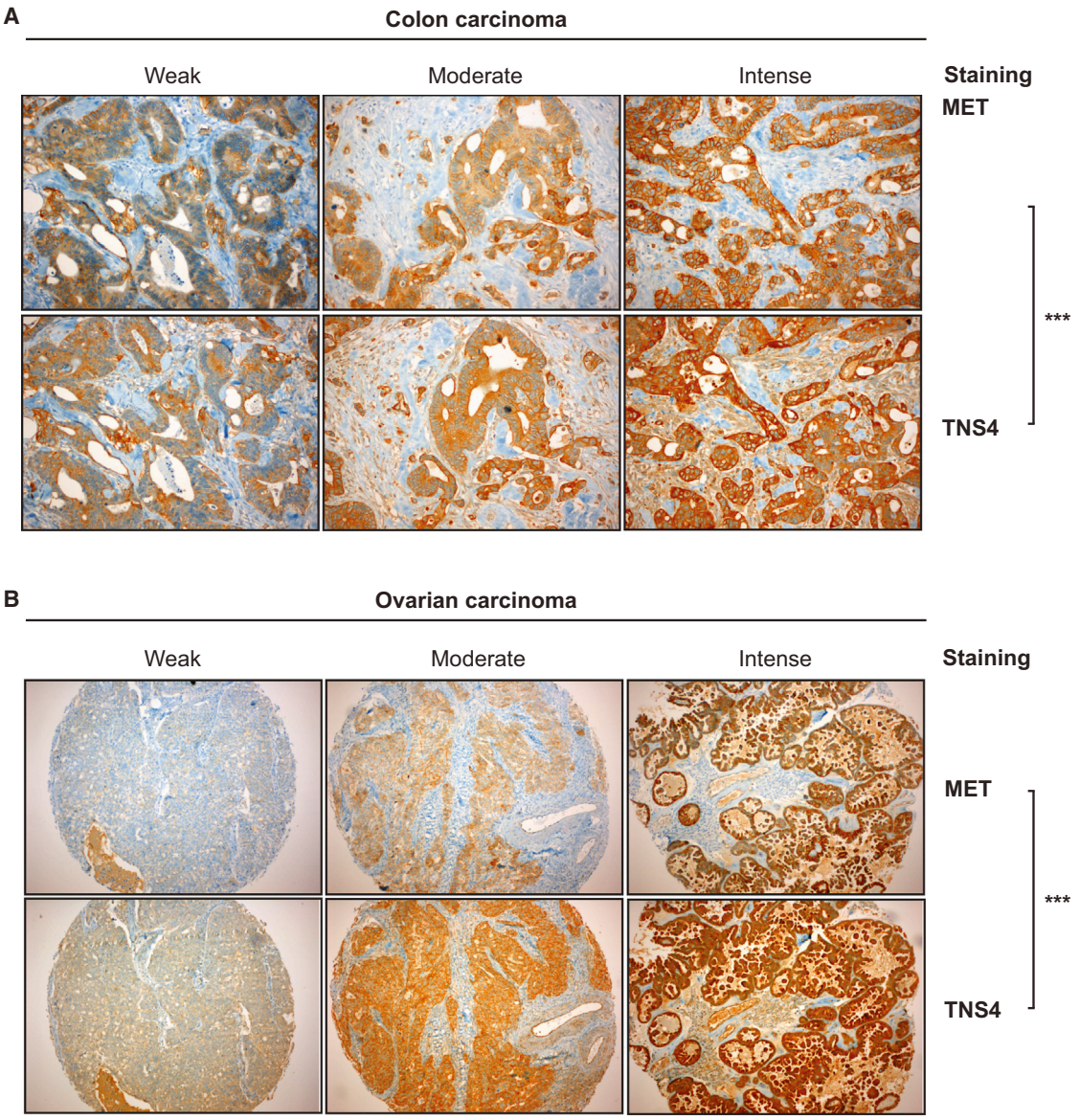

Tumor samples spotted	n = 124
Tumor cores stained	n = 196
Co-regulation overall samples	p < 0.0001
Excluding benign. borderline samples	p < 0.0001
Serous cystadenocarcinomas n= 49	p < 0.0001
Mucinous cystadenocarcinoma n= 39	p = 0.012
Endometrioid cystadenocarcinoma n= 43	p = 0.13

Figure 6. TNS4 and MET Are Coexpressed in the Same Areas of Colorectal and Ovarian Epithelial Tumors
(A) MET and TNS4 staining of adjacent colorectal cancer sections from the same tumor (magnification ×20).
(B) MET and TNS4 staining of adjacent sections of ovarian tumor tissue microarray spots (magnification ×10). ***$p < 0.0001$.

MesNa treatment. Cells were then washed with PBS, scraped in lysis buffer (1.5% octylglucoside, 1% NP-40, 0.5% BSA, 1 mM EDTA with phosphatase and protease inhibitor cocktail tablets [Roche]) at 4°C for 20 min. In recycling experiments, following the first MesNA/IAA treatment, the cells were returned to prewarmed 10% serum-containing medium at 37°C for the indicated times and treated again with MesNa/IAA to remove biotin from the cell-surface recycled receptor. All cell extracts were cleared by centrifugation (14,000 × g, 10 min, 4°C), and biotinylated MET or integrin were immunoprecipitated

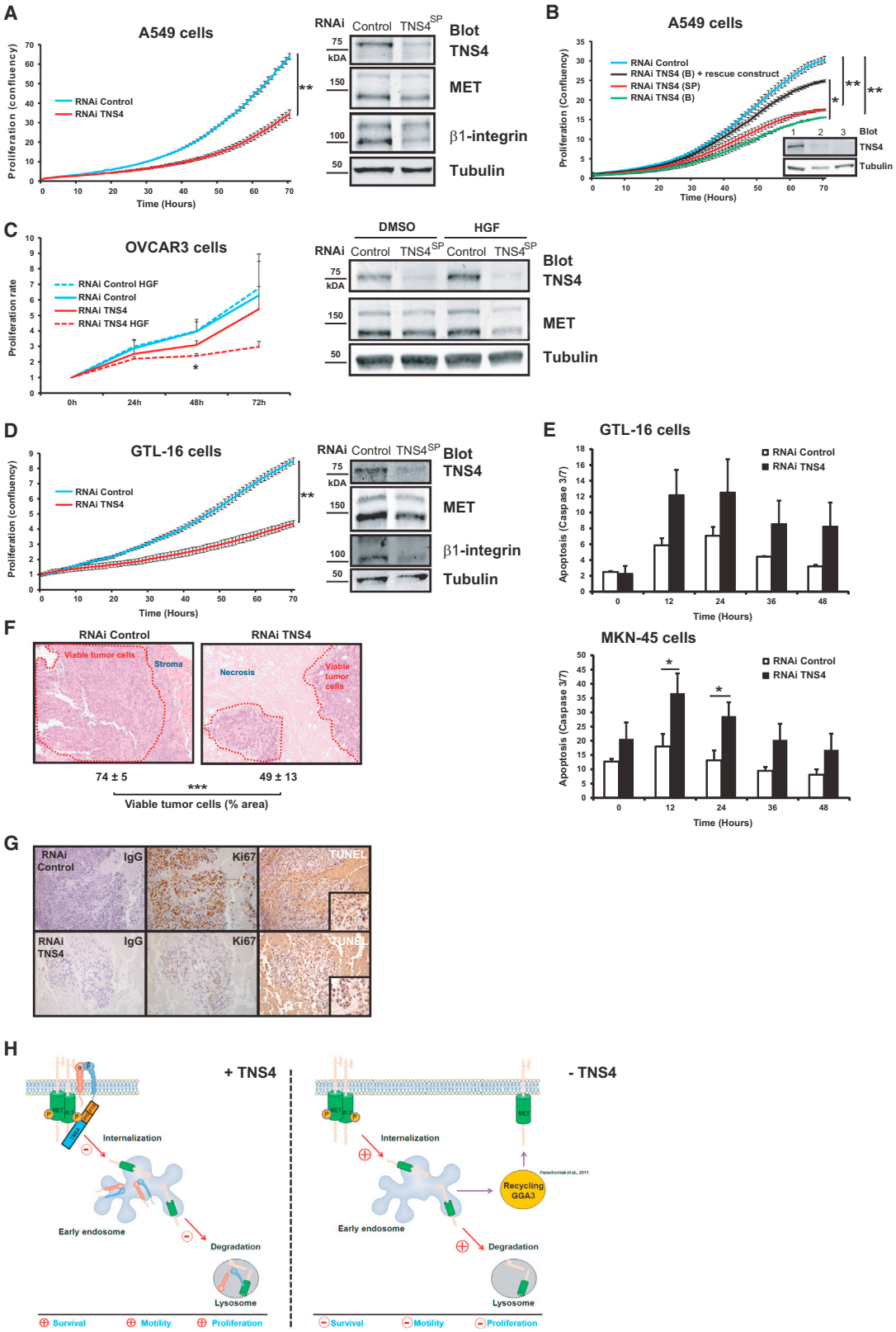

(legend on next page)

from the supernatants with appropriate antibodies and protein G sepharose beads (17-0618-01; GE Healthcare).

Biotinylated internalized MET and β1-integrin receptors and total receptor levels were detected by immunoblotting with horseradish peroxidase (HRP)-conjugated anti-biotin antibody (#7075; Cell Signaling Technology) and receptor-specific antibodies, respectively.

Enhanced chemiluminescence-detected biotin and receptor signals were quantified as integrated densities of protein bands with ImageJ (v. 1.43u), and each biotin signal was normalized to the corresponding receptor and total biotin signal. The endocytosis rate of MET was similarly measured in control- or TNS4-silenced cells.

Animal Studies

Experimental procedures were approved by the Committee for Care and Use of Animals in Experiments at the University of Turku and the State Provincial office of Western Finland (authorization ESLM-2008-08600). TNS4- or control-silenced GTL-16 cells (2.10^6) were subcutaneously injected in one flank of ten athymic nude mice (5–6 weeks old females, Harlan) for each cell type. Mice were sacrificed 12 days after injection. Tumors were removed and fixed in formalin before paraffin inclusion. All tumor sections were stained for hematoxylin and eosin to quantify viable tumoral tissue. For Ki67 and TUNEL staining, tumor sections from three mice in each group were compared.

Immunohistochemical Staining of Human Tumor Samples

Tumor sections were formalin fixed, paraffin embedded, and stained with antibodies against TNS4 and MET using Ventana BenchMark XT (Ventana Medical Systems, Roche Diagnostics). See the Supplemental Experimental Procedures for detailed staining and scoring protocols.

In Vitro Proliferation and Survival Assay

Cells were imaged in an IncuCyteHD (Essen Instruments) automated incubator microscope, and cell confluence was calculated per well by associated software algorithm (Haapa-Paananen et al., 2012). WST-1 in vitro proliferation assay (Roche) was used to measure A549 and OVCAR3 cells proliferation. Apoptosis was measured using DEVD 488 Nucview substrate (1 μM, Essen BioScience) of caspase-3/7. For further details, see the Supplemental Experimental Procedures.

SUPPLEMENTAL INFORMATION

Supplemental Information includes Supplemental Experimental Procedures, six figures, one table, and two movies and can be found with this article online at http://dx.doi.org/10.1016/j.devcel.2014.03.024.

AUTHOR CONTRIBUTIONS

G.M. designed and performed experiments, analyzed data, and wrote the paper; P.S. and T.K. contributed equally; P.S. performed and analyzed the trafficking experiments, and T.K. performed and analyzed the histology staining. N.D.F. performed the sequence analysis and structural modeling. R.K. assisted with the cell-derived matrix experiments. K.C. and D.T. provided research tools, expertise, and help with the protein-interaction studies. The yeast two-hybrid experiments were carried out in D.T.'s laboratory. O.C. designed the experiments related to the clinical material, analyzed data, and contributed to writing the paper. J.I. designed and performed experiments, discussed data, and wrote the paper.

ACKNOWLEDGMENTS

The authors are very grateful for technical assistance from J. Nevo, E. Mattila, L. Lahtinen, J. Siivonen, and P. Laasola. Dr. H. Hamidi is acknowledged for scientific writing, and Professor J. Westermarck is acknowledged for critically reading the manuscript. Professor D. Critchley (University of Leicester) is acknowledged for support in generating Tensin constructs and TNS3 antibody. Dr. G. Serini (University of Torino) is acknowledged for providing Lamp1-RFP construct. K.C. has been funded by the Wellcome Trust. P.S. is funded by the Turku Doctoral program of Molecular Medicine (TuDMM). This study has been supported by the Academy of Finland, an ERC Starting Grant, an ERC Consolidator Grant, the Sigrid Juselius Foundation, and the Finnish Cancer Organizations.

Received: June 7, 2013
Revised: February 5, 2014
Accepted: March 31, 2014
Published: May 8, 2014

REFERENCES

Al-Ghamdi, S., Albasri, A., Cachat, J., Ibrahem, S., Muhammad, B.A., Jackson, D., Nateri, A.S., Kindle, K.B., and Ilyas, M. (2011). Cten is targeted by Kras signalling to regulate cell motility in the colon and pancreas. PLoS ONE *6*, e20919.

Albasri, A., Seth, R., Jackson, D., Benhasouna, A., Crook, S., Nateri, A.S., Chapman, R., and Ilyas, M. (2009). C-terminal Tensin-like (CTEN) is an oncogene which alters cell motility possibly through repression of E-cadherin in colorectal cancer. J. Pathol. *218*, 57–65.

Ålgars, A., Lintunen, M., Carpén, O., Ristamäki, R., and Sundström, J. (2011). EGFR gene copy number assessment from areas with highest EGFR

Figure 7. TNS4 Silencing Induces MET Downregulation Associated with Reduced Cell Proliferation and Survival In Vitro and In Vivo

(A) Proliferation of control- or TNS4-silenced (SP) A549 cells analyzed by IncuCyteHD incubator microscope (mean confluence values were compared at 70 hr; n = 5). Corresponding cell lysates were analyzed by western blot.

(B) Proliferation of A549 cells transfected with either control or TNS4 siRNAs (SP or single TNS4 RNAi B) ± TNS4-SH2-PTB-GFP rescue construct as analyzed by IncuCyteHD incubator microscope (mean confluence values were compared at 70 hr; n = 3). Western blot shows TNS4 silencing efficiency (lane 1: control-silenced cell extracts; lane 2: TNS4 SP; lane 3: TNS4 RNAi B).

(C) WST-1 proliferation assay of control- or TNS4 (SP)-silenced OVCAR3 cells ± HGF (5 ng/ml) (mean ± SEM; absorbance normalized to day 1 values; n = 3). Statistical significance was analyzed at each time point between untreated control- versus TNS4-silenced cells (nonsignificant) or HGF-stimulated control- versus HGF-treated TNS4-silenced cells at the indicated time point (*$p < 0.05$). Corresponding cell lysates were analyzed by western blot.

(D) Proliferation of control- or TNS4-silenced GTL-16 cells analyzed with IncuCyteHD (mean confluence values were compared at 70 hr; n = 3). Corresponding cell lysates were analyzed by western blot.

(E) Apoptosis of control- or TNS4-silenced GTL-16 and MKN-45 cells detected using DEVD-488 Nucview Caspase3/7 substrate in IncuCyteFLR incubator microscope. Shown are fluorescent apoptotic cell counts (normalized to cell confluence per well; mean ± SEM; n = 2–3).

(F) Quantification of tumor viability in xenograft sections of transplanted GTL-16 cells (n = 10 mice per group). Viable cells are outlined in representative images (magnification ×10). *$p < 0.05$, **$p < 0.005$,***$p < 0.0001$.

(G) Ki67, TUNEL, and IgG (negative control) staining of tumor sections used in (F).

(H) Proposed model: TNS4 interacts with β1-integrin and MET to inhibit internalization and subsequent degradation of both receptors. TNS4-dependent high MET expression correlates with sustained MET signaling and increased cancer cell survival, motility, and proliferation. Suppression of TNS4 expression (right panel) results in increased MET internalization and either subsequent MET recycling back to the cell surface in a HGF-activation-dependent manner (Parachoniak et al., 2011) via the previously described GGA3 pathway or leads to increased lysosomal degradation associated with decreased MET levels and downstream signaling.

expression predicts response to anti-EGFR therapy in colorectal cancer. Br. J. Cancer *105*, 255–262.

Arjonen, A., Alanko, J., Veltel, S., and Ivaska, J. (2012). Distinct recycling of active and inactive β1 integrins. Traffic *13*, 610–625.

Bertotti, A., Bracco, C., Girolami, F., Torti, D., Gastaldi, S., Galimi, F., Medico, E., Elvin, P., Comoglio, P.M., and Trusolino, L. (2010). Inhibition of Src impairs the growth of met-addicted gastric tumors. Clin. Cancer Res. *16*, 3933–3943.

Birchmeier, C., Birchmeier, W., Gherardi, E., and Vande Woude, G.F. (2003). Met, metastasis, motility and more. Nat. Rev. Mol. Cell Biol. *4*, 915–925.

Blumenschein, G.R., Jr., Mills, G.B., and Gonzalez-Angulo, A.M. (2012). Targeting the hepatocyte growth factor-cMET axis in cancer therapy. J. Clin. Oncol. *30*, 3287–3296.

Calderwood, D.A., Fujioka, Y., de Pereda, J.M., García-Alvarez, B., Nakamoto, T., Margolis, B., McGlade, C.J., Liddington, R.C., and Ginsberg, M.H. (2003). Integrin beta cytoplasmic domain interactions with phosphotyrosine-binding domains: a structural prototype for diversity in integrin signaling. Proc. Natl. Acad. Sci. USA *100*, 2272–2277.

Chen, N.T., Kuwabara, Y., Conley, C., Liao, Y.C., Hong, S.Y., Chen, M., Shih, Y.P., Chen, H.W., Hsieh, F., and Lo, S.H. (2013). Phylogenetic analysis, expression patterns, and transcriptional regulation of human CTEN gene. Gene *520*, 90–97.

Clark, K., Howe, J.D., Pullar, C.E., Green, J.A., Artym, V.V., Yamada, K.M., and Critchley, D.R. (2010). Tensin 2 modulates cell contractility in 3D collagen gels through the RhoGAP DLC1. J. Cell. Biochem. *109*, 808–817.

Cui, Y., Liao, Y.C., and Lo, S.H. (2004). Epidermal growth factor modulates tyrosine phosphorylation of a novel tensin family member, tensin3. Mol. Cancer Res. *2*, 225–232.

Defilippi, P., Di Stefano, P., and Cabodi, S. (2006). p130Cas: a versatile scaffold in signaling networks. Trends Cell Biol. *16*, 257–263.

Garcia-Echeverria, C., Stamm, C., Wille, R., Arz, D., and Gay, B. (1997). Biotinylated phosphotyrosine containing peptides: a valuable tool for studies on phosphopeptide interactions with SH2 and PTB domains. Lett. Pept. Sci. *4*, 49–53.

Gherardi, E., Birchmeier, W., Birchmeier, C., and Vande Woude, G. (2012). Targeting MET in cancer: rationale and progress. Nat. Rev. Cancer *12*, 89–103.

Goodman, S.L., and Picard, M. (2012). Integrins as therapeutic targets. Trends Pharmacol. Sci. *33*, 405–412.

Haapa-Paananen, S., Kiviluoto, S., Waltari, M., Puputti, M., Mpindi, J.P., Kohonen, P., Tynninen, O., Haapasalo, H., Joensuu, H., Perälä, M., and Kallioniemi, O. (2012). HES6 gene is selectively overexpressed in glioma and represents an important transcriptional regulator of glioma proliferation. Oncogene *31*, 1299–1310.

Hammond, D.E., Urbé, S., Vande Woude, G.F., and Clague, M.J. (2001). Down-regulation of MET, the receptor for hepatocyte growth factor. Oncogene *20*, 2761–2770.

Hammond, D.E., Carter, S., McCullough, J., Urbé, S., Vande Woude, G., and Clague, M.J. (2003). Endosomal dynamics of Met determine signaling output. Mol. Biol. Cell *14*, 1346–1354.

Hong, S.Y., Shih, Y.P., Li, T., Carraway, K.L., 3rd, and Lo, S.H. (2013). CTEN prolongs signaling by EGFR through reducing its ligand-induced degradation. Cancer Res. *73*, 5266–5276.

Houldsworth, J., Cordon-Cardo, C., Ladanyi, M., Kelsen, D.P., and Chaganti, R.S. (1990). Gene amplification in gastric and esophageal adenocarcinomas. Cancer Res. *50*, 6417–6422.

Huang, H., Li, L., Wu, C., Schibli, D., Colwill, K., Ma, S., Li, C., Roy, P., Ho, K., Songyang, Z., et al. (2008). Defining the specificity space of the human SRC homology 2 domain. Mol. Cell. Proteomics *7*, 768–784.

Ivaska, J., and Heino, J. (2011). Cooperation between integrins and growth factor receptors in signaling and endocytosis. Annu. Rev. Cell Dev. Biol. *27*, 291–320.

Joffre, C., Barrow, R., Ménard, L., Calleja, V., Hart, I.R., and Kermorgant, S. (2011). A direct role for Met endocytosis in tumorigenesis. Nat. Cell Biol. *13*, 827–837.

Katz, M., Amit, I., Citri, A., Shay, T., Carvalho, S., Lavi, S., Milanezi, F., Lyass, L., Amariglio, N., Jacob-Hirsch, J., et al. (2007). A reciprocal tensin-3-cten switch mediates EGF-driven mammary cell migration. Nat. Cell Biol. *9*, 961–969.

Kermorgant, S., Zicha, D., and Parker, P.J. (2004). PKC controls HGF-dependent c-Met traffic, signalling and cell migration. EMBO J. *23*, 3721–3734.

Kwon, S.H., Nedvetsky, P.I., and Mostov, K.E. (2011). Transcriptional profiling identifies TNS4 function in epithelial tubulogenesis. Curr. Biol. *21*, 161–166.

Lai, A.Z., Abella, J.V., and Park, M. (2009). Crosstalk in Met receptor oncogenesis. Trends Cell Biol. *19*, 542–551.

Lefebvre, J., Ancot, F., Leroy, C., Muharram, G., Lemière, A., and Tulasne, D. (2012). Met degradation: more than one stone to shoot a receptor down. FASEB J. *26*, 1387–1399.

Legate, K.R., and Fässler, R. (2009). Mechanisms that regulate adaptor binding to beta-integrin cytoplasmic tails. J. Cell Sci. *122*, 187–198.

Liao, Y.C., Si, L., deVere White, R.W., and Lo, S.H. (2007). The phosphotyrosine-independent interaction of DLC-1 and the SH2 domain of cten regulates focal adhesion localization and growth suppression activity of DLC-1. J. Cell Biol. *176*, 43–49.

Liao, Y.C., Chen, N.T., Shih, Y.P., Dong, Y., and Lo, S.H. (2009). Up-regulation of C-terminal tensin-like molecule promotes the tumorigenicity of colon cancer through beta-catenin. Cancer Res. *69*, 4563–4566.

Lo, S.H. (2007). Reverse interactomics: from peptides to proteins and to functions. ACS Chem. Biol. *2*, 93–95.

Lo, S.H., and Lo, T.B. (2002). Cten, a COOH-terminal tensin-like protein with prostate restricted expression, is down-regulated in prostate cancer. Cancer Res. *62*, 4217–4221.

Lutterbach, B., Zeng, Q., Davis, L.J., Hatch, H., Hang, G., Kohl, N.E., Gibbs, J.B., and Pan, B.S. (2007). Lung cancer cell lines harboring MET gene amplification are dependent on Met for growth and survival. Cancer Res. *67*, 2081–2088.

Mai, A., Veltel, S., Pellinen, T., Padzik, A., Coffey, E., Marjomäki, V., and Ivaska, J. (2011). Competitive binding of Rab21 and p120RasGAP to integrins regulates receptor traffic and migration. J. Cell Biol. *194*, 291–306.

McCleverty, C.J., Lin, D.C., and Liddington, R.C. (2007). Structure of the PTB domain of tensin1 and a model for its recruitment to fibrillar adhesions. Protein Sci. *16*, 1223–1229.

Mitra, S.K., and Schlaepfer, D.D. (2006). Integrin-regulated FAK-Src signaling in normal and cancer cells. Curr. Opin. Cell Biol. *18*, 516–523.

Muller, P.A., Trinidad, A.G., Timpson, P., Morton, J.P., Zanivan, S., van den Berghe, P.V., Nixon, C., Karim, S.A., Caswell, P.T., Noll, J.E., et al. (2013). Mutant p53 enhances MET trafficking and signalling to drive cell scattering and invasion. Oncogene *32*, 1252–1265.

Parachoniak, C.A., Luo, Y., Abella, J.V., Keen, J.H., and Park, M. (2011). GGA3 functions as a switch to promote Met receptor recycling, essential for sustained ERK and cell migration. Dev. Cell *20*, 751–763.

Peschard, P., Fournier, T.M., Lamorte, L., Naujokas, M.A., Band, H., Langdon, W.Y., and Park, M. (2001). Mutation of the c-Cbl TKB domain binding site on the Met receptor tyrosine kinase converts it into a transforming protein. Mol. Cell *8*, 995–1004.

Qian, X., Li, G., Vass, W.C., Papageorge, A., Walker, R.C., Asnaghi, L., Steinbach, P.J., Tosato, G., Hunter, K., and Lowy, D.R. (2009). The Tensin-3 protein, including its SH2 domain, is phosphorylated by Src and contributes to tumorigenesis and metastasis. Cancer Cell *16*, 246–258.

Roberts, M., Barry, S., Woods, A., van der Sluijs, P., and Norman, J. (2001). PDGF-regulated rab4-dependent recycling of alphavbeta3 integrin from early endosomes is necessary for cell adhesion and spreading. Curr. Biol. *11*, 1392–1402.

Rong, S., Segal, S., Anver, M., Resau, J.H., and Vande Woude, G.F. (1994). Invasiveness and metastasis of NIH 3T3 cells induced by Met-hepatocyte growth factor/scatter factor autocrine stimulation. Proc. Natl. Acad. Sci. USA *91*, 4731–4735.

Sakashita, K., Mimori, K., Tanaka, F., Kamohara, Y., Inoue, H., Sawada, T., Hirakawa, K., and Mori, M. (2008). Prognostic relevance of Tensin4 expression in human gastric cancer. Ann. Surg. Oncol. *15*, 2606–2613.

Sasaki, H., Moriyama, S., Mizuno, K., Yukiue, H., Konishi, A., Yano, M., Kaji, M., Fukai, I., Kiriyama, M., Yamakawa, Y., and Fujii, Y. (2003a). Cten mRNA expression was correlated with tumor progression in lung cancers. Lung Cancer *40*, 151–155.

Sasaki, H., Yukiue, H., Kobayashi, Y., Fukai, I., and Fujii, Y. (2003b). Cten mRNA expression is correlated with tumor progression in thymoma. Tumour Biol. *24*, 271–274.

Smolen, G.A., Sordella, R., Muir, B., Mohapatra, G., Barmettler, A., Archibald, H., Kim, W.J., Okimoto, R.A., Bell, D.W., Sgroi, D.C., et al. (2006). Amplification of MET may identify a subset of cancers with extreme sensitivity to the selective tyrosine kinase inhibitor PHA-665752. Proc. Natl. Acad. Sci. USA *103*, 2316–2321.

Straussman, R., Morikawa, T., Shee, K., Barzily-Rokni, M., Qian, Z.R., Du, J., Davis, A., Mongare, M.M., Gould, J., Frederick, D.T., et al. (2012). Tumour micro-environment elicits innate resistance to RAF inhibitors through HGF secretion. Nature *487*, 500–504.

Trusolino, L., Bertotti, A., and Comoglio, P.M. (2010). MET signalling: principles and functions in development, organ regeneration and cancer. Nat. Rev. Mol. Cell Biol. *11*, 834–848.

Zhou, H.Y., Pon, Y.L., and Wong, A.S. (2008). HGF/MET signaling in ovarian cancer. Curr. Mol. Med. *8*, 469–480.

Zou, H.Y., Li, Q., Lee, J.H., Arango, M.E., McDonnell, S.R., Yamazaki, S., Koudriakova, T.B., Alton, G., Cui, J.J., Kung, P.P., et al. (2007). An orally available small-molecule inhibitor of c-Met, PF-2341066, exhibits cytoreductive antitumor efficacy through antiproliferative and antiangiogenic mechanisms. Cancer Res. *67*, 4408–4417.